

COSMIC EVOLUTION IN A BIANCHI TYPE-V UNIVERSE WITH BARROW HOLOGRAPHIC DARK ENERGY WITH GRANDA-OLIVEROS LENGTH SCALE AS IR CUTOFF

 Chandra Rekha Mahanta,  Rajashree Mahanta*,  Joy Prakash Medhi

Department of Mathematics, Gauhati University, Guwahati - 781014 (INDIA)

*Corresponding Author e-mail: rajashree.mahanta@gauhati.ac.in

Received June 30, 2024; revised July 26, 2024; accepted August 5, 2024

In this work, we construct a spatially homogeneous and anisotropic Bianchi type-V cosmological model with a hybrid expansion law by considering the universe to be filled with cold dark matter and non-interacting Barrow holographic dark energy with Granda-Oliveros length scale as IR cutoff. The physical and kinematical characteristics of the resulting model are discussed by studying the evolution of various parameters of cosmological importance such as the Hubble parameter, the deceleration parameter, the anisotropic parameter, the equation of state parameter, jerk parameter etc. We also examine whether the energy conditions are satisfied or violated. Our analysis reveals that the Null, Weak, and Dominant energy conditions are fulfilled, while the Strong Energy Condition is violated, which supports the accelerated expansion of the universe. Statefinder diagnostics have also been performed based on recent cosmological observations in order to compare our model with different dark energy cosmological scenario. Additionally, we establish the correspondence between the quintessence scalar field and the Barrow holographic dark energy model, supporting our description of the universe's accelerated expansion.

Keywords: *Cosmic acceleration; Barrow holographic dark energy; Bianchi type-V; Cold dark matter; Deceleration parameter; Equation of state parameter*

PACS: 95.35.+d, 95.36.+x, 98.80.-k, 98.80.Jk, 98.80.Es, 04.20.Jb

1. INTRODUCTION

In the late twentieth century, the observational data from two independent projects, the High-redshift Supernova Search Team led by A. G. Riess [1] and the Supernova Cosmology Project led by S. Perlmutter [2], revealed that the universe is currently in a phase of accelerated expansion. Since then, various astrophysical and cosmological observations such as the temperature anisotropies in the Cosmic Microwave Background (CMB) [3, 4, 5], Large Scale Structure (LSS) such as the galaxy clustering [6, 7, 8], Baryon Acoustic Oscillations (BAO) [9] etc. have been supporting the observed acceleration. The root cause or the source for this bizarre late-time cosmic acceleration has not been identified yet and it remains as a great challenge in modern cosmology even after more than two decades of its discovery. Most of the cosmological models presented in the literature attribute the cosmic acceleration to a component with negative pressure, commonly referred to as dark energy, an enigmatic form of physical entity that dominates the universe and is causing the current universe to enter into an accelerated phase of expansion. The observational data also show that the combined dark components accounts for around 95% of the universe's total energy density, with dark matter (DM), a non-relativistic matter that interacts very weakly with baryonic *i.e.* standard matter particles, contributing about 27% and dark energy (DE) contributing approximately 68% of the entire matter-energy allocation, and only about 5% is ordinary baryonic matter, the most basic model being the concordance model, popularly known as the Λ CDM model, in which dark energy is represented by the cosmological constant Λ , introduced by Einstein in his field equations, although it needs to be fine-tuned to fit the available observational data [10, 11]. As a result, a variety of dynamically evolving scalar field models such as quintessence, k-essence, tachyon, quintom, dilatonic ghost condensate, phantom etc. and exotic fluid models like Chaplygin gas models [12] are proposed in the literature.

Recently, attention has been drawn to a number of holographic dark energy models initially originating from the Holographic Principle proposed by G't Hooft [13] in the context of black hole physics, and on the hypothesis [14] on the mutual relationship between the short distance UV cutoff and IR cutoff. However, the original holographic dark energy models [15, 16, 17] constructed by attributing Bekenstein-Hawking entropy and Hubble horizon could not provide satisfactory explanation for the current accelerated expansion. The density of holographic dark energy, as determined by Li's work [17], is $\rho_D = 3c^2 M_P^2 L^{-2}$, where L is the infrared (IR) cutoff, M_P is the Planck mass and $3c^2$ is a numerical constant. Various appropriate choice of this IR cutoff result in new cosmological problems. The Granda and Oliveros cutoff [18] is utilized in proposing a new holographic dark energy (NHDE) model, where the energy density is expressed as the square of the Hubble parameter and its time derivative. The Tsallis holographic dark energy (THDE) model was developed in 2018 [19] using the Tsallis generalized entropy $S_\delta = \gamma A^\delta$, where δ is a non-additive parameter, A is the event horizon's surface area and γ is a constant [20]. Another holographic dark energy model, known as the Rényi holographic

dark energy (RHDE), was formulated utilizing the Rényi entropy [21]. Barrow [22] has suggested a new approach to black hole entropy, incorporating quantum gravitational effects. This could potentially introduce intricate and fractal properties to the black hole's area, represented by $S_B = \left(\frac{A}{A_0}\right)^{1+\frac{\Delta}{2}}$, where A is the standard horizon area, A_0 is the Planck area, and the exponent Δ , ranging from 0 to 1, quantifies the quantum gravitational deformation. When Δ equals 1, the structure exhibits maximal complexity and fractal characteristics, whereas when Δ equals 0, it corresponds to the standard Bekenstein-Hawking entropy or the standard smooth structure. The standard holographic dark energy density is defined by the inequality $\rho_{HDE} L^4 \leq S$, where ' L ' represents the horizon length. When subjected to the condition $S \propto A \propto L^2$ [23], the Barrow entropy provides the energy density for Barrow holographic dark energy (BHDE) as $\rho_{BHDE} = 3c^2 M_p^2 L^{\Delta-2}$, where ' c^2 ' is the model parameter and ' M_p ' is the Planck mass. Saridakis [24] innovated the BHDE by utilizing the Barrow entropy rather than the standard Bekenstein-Hawking entropy. Furthermore, Srivastava and Sharma [25] explore the flat Friedmann-Lemaître-Robertson-Walker (FLRW) universe by employing the BHDE with the Hubble horizon as the infrared cutoff. The authors in [26], recently investigated the Barrow holographic dark energy with the Granda-Oliveros length serving as the infrared cutoff. The authors in [27] investigated Barrow holographic dark energy within a flat Friedmann-Lemaître-Robertson-Walker (FLRW) universe, employing the Granda-Oliveros length as the infrared cutoff and determined the impact of the deformation parameter Δ on the evolution of $H(z)$. When Paul *et al.* [28] examined the Bianchi type-I universe in the presence of BHDE, they found that the new exponent is crucial in determining the nature of the universe.

The Friedmann-Lemaître-Robertson-Walker model characterizes the universe as homogeneous and isotropic on a large scale. But it is essential to note that there is no observable evidence definitively excluding the existence of an anisotropic universe. Anisotropic cosmological models [29, 30, 31] have gained prominence due to observations of the Cosmic Microwave Background Radiation (CMBR) and the formation of Helium in the early stages of the universe's evolution. The presence of anisotropy in cosmic expansion is a significant factor, supported by critical arguments and experimental data suggesting the existence of an anisotropic phase transitioning towards isotropy over time. Hence, it is crucial to consider models incorporating an anisotropic background. Spatially homogeneous and anisotropic Bianchi models are commonly taken into consideration to gain a better understanding of the dynamics of the expanding universe. This is because they are the most basic models with an anisotropic background and are important in explaining the large-scale behavior of the universe. In order to properly connect the homogeneous and isotropic FLRW models with the inhomogeneous and anisotropic models, Bianchi type models provide means of incorporating the influence of anisotropy. As a result, a large number of scholars have investigated anisotropic and spatially homogeneous Bianchi cosmological models in many contexts.

In this study, we develop a cosmological model of Bianchi type-V, which is both spatially homogeneous and anisotropic. This model incorporates a hybrid expansion law, assuming the universe to be filled with cold dark matter and non-interacting Barrow holographic dark energy with the Granda-Oliveros length scale serving as the IR cutoff. The paper is structured in the following manner: In section 2, we derive the Einstein field equations for the Bianchi type-V metric. In Section 3, exact solutions to the field equations are obtained by employing a hybrid expansion law. Furthermore, we consider several cosmologically relevant parameters. In section 4, we examine the model's kinematical and physical characteristics as well as its energy conditions. In Section 5, we explore the Statefinder diagnostics and examine its consequences. In Section 6, we explore the correlation between BHDE and a quintessence scalar field. In Section 7, we provide concluding remarks on our findings.

2. THE METRIC AND BASIC FIELD EQUATIONS

We consider the spatially homogeneous and anisotropic Bianchi type-V universe characterised by the metric:

$$ds^2 = -dt^2 + A^2 dx^2 + e^{2\eta x} \{B^2 dy^2 + C^2 dz^2\} \quad (1)$$

where η is a positive constant and $A(t)$, $B(t)$ and $C(t)$ are the directional scale factors with t being the cosmic time.

With natural units of ($8\pi G = 1, c = 1$), the Einstein field equations are given by

$$R_{ij} - \frac{1}{2} g_{ij} R = T_{ij} \quad (2)$$

where R_{ij} is the Ricci tensor, g_{ij} is the metric tensor, $R = g^{ij} R_{ij}$ is the Ricci scalar curvature and T_{ij} is the energy momentum tensor of the cosmic fluid.

We consider the universe to be filled with a mixture of pressureless cold dark matter and non-interacting Barrow holographic dark energy with Granda Oliveros (GO) length scale as IR cutoff given by

$$\rho_{BHDE} = 3 \left(\alpha H^2 + \beta \dot{H} \right)^{\frac{2-\Delta}{2}} \quad (3)$$

where ρ_{BHDE} is the energy density of Barrow holographic dark energy (BHDE) and $[L]^{\frac{-2\Delta}{2-\Delta}}$ is the dimension of the

constant parameters α and β . H represents the Hubble parameter.

The energy-momentum tensor T_{ij} can be written as

$$T_{ij} = \rho_m u_i u_j + (\rho_{BHDE} + p_{BHDE}) u_i u_j + g_{ij} p_{BHDE} \tag{4}$$

where ρ_m represents the energy density of cold dark matter, ρ_{BHDE} and p_{BHDE} are the energy density and pressure of Barrow holographic dark energy, respectively and u_i is the four velocity satisfying $u^i u_i = -1$.

In a comoving coordinate system, the Einstein field equations (2), along with equation (4) for the metric (1), result in the following system of field equations:

$$\frac{\ddot{B}}{B} + \frac{\ddot{C}}{C} + \frac{\dot{B}\dot{C}}{BC} - \frac{\eta^2}{A^2} = -p_{BHDE} \tag{5}$$

$$\frac{\ddot{A}}{A} + \frac{\ddot{C}}{C} + \frac{\dot{A}\dot{C}}{AC} - \frac{\eta^2}{A^2} = -p_{BHDE} \tag{6}$$

$$\frac{\ddot{A}}{A} + \frac{\ddot{B}}{B} + \frac{\dot{A}\dot{B}}{AB} - \frac{\eta^2}{A^2} = -p_{BHDE} \tag{7}$$

$$\frac{\dot{A}\dot{B}}{AB} + \frac{\dot{A}\dot{C}}{AC} + \frac{\dot{B}\dot{C}}{BC} - \frac{3\eta^2}{A^2} = \rho_m + \rho_{BHDE} \tag{8}$$

$$\frac{2\dot{A}}{A} - \frac{\dot{B}}{B} - \frac{\dot{C}}{C} = 0 \tag{9}$$

where a dot above indicates a differentiation with respect to t .

From equation (9), we obtain:

$$A^2 = BC \tag{10}$$

The conservation of energy-momentum yields

$$\dot{\rho}_m + \dot{\rho}_{BHDE} + 3H(\rho_m + \rho_{BHDE} + p_{BHDE}) = 0 \tag{11}$$

We can divide equation (11) into the following two continuity equations as the BHDE and cold dark matter are non-interacting:

$$\dot{\rho}_m + 3H\rho_m = 0 \tag{12}$$

$$\dot{\rho}_{BHDE} + 3H(\rho_{BHDE} + p_{BHDE}) = 0 \tag{13}$$

3. COSMOLOGICAL SOLUTIONS OF THE FIELD EQUATIONS

From Einstein's field equations (5) – (8), we obtain:

$$\frac{A}{B} = d_1 e^{k_1 \int a^{-3} dt} \tag{14}$$

$$\frac{A}{C} = d_2 e^{k_2 \int a^{-3} dt} \tag{15}$$

$$\frac{B}{C} = d_3 e^{k_3 \int a^{-3} dt} \tag{16}$$

where $d_1, d_2, d_3, k_1, k_2, k_3$ are the constants of integration and a is the average scale defined by.

$$a = (ABC)^{\frac{1}{3}} \tag{17}$$

which parameterizes the universe's relative expansion.

The metric functions from equations (14) – (16) and (10) can be directly obtained as

$$A = a \quad (18)$$

$$B = ma e^{l \int a^{-3} dt} \quad (19)$$

$$C = \frac{a}{m} e^{-l \int a^{-3} dt} \quad (20)$$

$$\text{where } m = (d_2 d_3)^{\frac{1}{3}}, \quad l = \frac{k_2 + k_3}{3}, \quad d_2 = d_1^{-1}, \quad k_2 = -k_1 \quad (21)$$

To derive a complete solution for the field equations, we take into account a hybrid expansion law in the form:

$$a = a_0 \left(t^k e^t \right)^{\frac{1}{n}} \quad (22)$$

where a_0 , k and n are positive constants.

Using (22) in (18), (19), (20), we then obtain

$$A = a_0 \left(t^k e^t \right)^{\frac{1}{n}} \quad (23)$$

$$B = ma_0 \left(t^k e^t \right)^{\frac{1}{n}} e^{lF(t)} \quad (24)$$

$$C = \frac{a_0}{m} \left(t^k e^t \right)^{\frac{1}{n}} e^{-lF(t)} \quad (25)$$

where $F(t) = \int a_0 \left(t^k e^t \right)^{\frac{-3}{n}} dt$.

4. PHYSICAL AND KINEMATICAL PROPERTIES OF THE MODEL

In order to comprehend the universe's evolution, we now introduce a few cosmic parameters: the mean Hubble parameter H , which determines the universe's rate of expansion, the spatial volume V , the scalar expansion (θ), shear scalar (σ), average anisotropic parameter (A_m) defined for the metric(1) by

$$V = a^3 = ABC \quad (26)$$

$$H = \frac{1}{3} (H_1 + H_2 + H_3) \quad (27)$$

$$\theta = 3H \quad (28)$$

$$\sigma^2 = \frac{1}{3} \left[\left(\frac{\dot{A}}{A} \right)^2 + \left(\frac{\dot{B}}{B} \right)^2 + \left(\frac{\dot{C}}{C} \right)^2 - \frac{\dot{A}\dot{B}}{AB} - \frac{\dot{B}\dot{C}}{BC} - \frac{\dot{C}\dot{A}}{CA} \right] \quad (29)$$

$$A_m = \frac{1}{3} \sum_{i=1}^3 \left(\frac{H_i - H}{H} \right)^2 \quad (30)$$

where the directional Hubble parameters along the three spatial directions x , y , and z , are respectively, $H_1 = \frac{\dot{A}}{A}$, $H_2 = \frac{\dot{B}}{B}$, $H_3 = \frac{\dot{C}}{C}$.

The universe’s relative rate of expansion (or contraction) is measured by the expansion scalar θ , its deformation due to density fluctuations is measured by the shear scalar σ , and its divergence from isotropy is measured by the anisotropy parameter A_m .

The directional Hubble parameters and the mean Hubble parameter (H) are obtained for the metric in (1) as :

$$H_1 = \frac{\dot{A}}{A} = \frac{k+t}{nt} \tag{31}$$

$$H_2 = \frac{\dot{B}}{B} = \frac{k+t}{nt} + lF'(t) \tag{32}$$

$$H_3 = \frac{\dot{C}}{C} = \frac{k+t}{nt} - lF'(t) \tag{33}$$

$$H = \frac{1}{3} \left(\frac{\dot{A}}{A} + \frac{\dot{B}}{B} + \frac{\dot{C}}{C} \right) = \frac{k+t}{nt} \tag{34}$$

The evolution of the Hubble parameter (H) with respect to cosmic time t are shown in figure 1. We can see from the figure that, for all values of n and k , H diverges at $t = 0$ and then decreases with cosmic time t .

The deceleration parameter can be found as follows using the relation $q = \frac{-a\ddot{a}}{\dot{a}^2}$:

$$q = \frac{kn}{(k+t)^2} - 1 \tag{35}$$

The dynamics of deceleration parameter (q) is determined by the two free parameters, n and k , as shown in Figure 2. The universe is accelerating from the beginning for $n = 1, k = 1.5$ (Red solid line) and $n = 0.5, k = 1$ (Green solid line); but, for $n = 1.1, k = 1$ (Blue solid line) and $n = 1.05, k = 1$ (Black solid line), it is transitioning from an early decelerating phase to the current accelerating phase. It is noted that our model is transitioning from the deceleration phase to the acceleration phase for $0 < \frac{k}{n} < 1$. Furthermore, current SNIa data reveal that the universe is expanding and that the deceleration parameter’s value falls somewhere between the interval $-1 < q < 0$.

We select $n = 1.1$ and $k = 1$ for plotting the graphs of the cosmological parameters to study their behaviour as the universe evolves. This is the most appropriate choice as we are looking for a model that describes the universe from early decelerating phase to current accelerating phase.

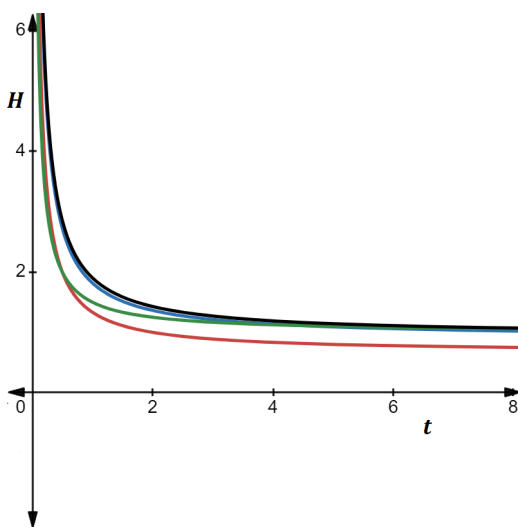


Figure 1. Plotting the Hubble parameter (H) vs cosmic time (t) for $n = 1, k = 1.5$ (Red solid line) , $n = 0.5, k = 1$ (Green solid line), $n = 1.1, k = 1$ (Blue solid line) and $n = 1.05, k = 1$ (Black solid line)

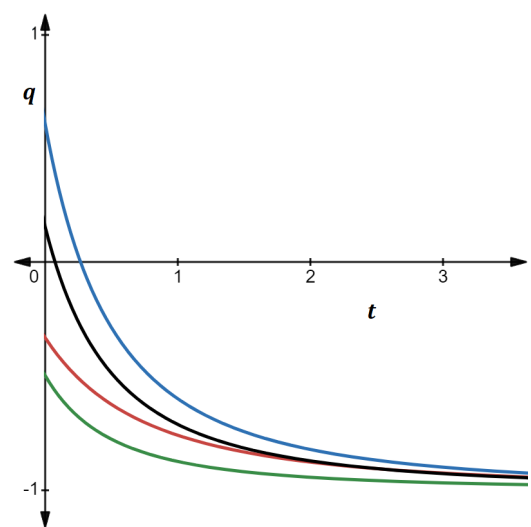


Figure 2. Plotting the deceleration parameter (DP) vs cosmic time (t) for $n = 1, k = 1.5$ (Red solid line) , $n = 0.5, k = 1$ (Green solid line), $n = 1.1, k = 1$ (Blue solid line) and $n = 1.05, k = 1$ (Black solid line)

For our model, the spatial volume V , shear scalar σ , expansion scalar θ , and average anisotropy parameter A_m are determined as follows:

$$V = a_0^3 \left(t^k e^t \right)^{\frac{3}{n}} \quad (36)$$

$$\sigma^2 = \frac{l^2}{\left(t^k e^t \right)^{\frac{6}{n}}} \quad (37)$$

$$\theta = 3 \left(\frac{k+t}{nt} \right) \quad (38)$$

$$A_m = \frac{2}{3} \frac{l^2 \left(t^k e^t \right)^{\frac{-6}{n}}}{\left(\frac{k+t}{nt} \right)^2} \quad (39)$$

From equations (36)–(39), we may infer that at the beginning of the universe, the spatial volume V is zero. Therefore, the Big Bang singularity is where our model begins. Both the shear scalar σ and the expansion scalar θ diverge at $t = 0$ and decrease as cosmic time t increases up to a fixed limit. The anisotropic parameter (A_m) varies with cosmic time, as seen in figure 3. It is demonstrated that for sufficiently long times, A_m diminishes with time and tends to zero for large t . As a result, the universe's anisotropic behavior eventually ends, and the derived model can produce the universe's observed isotropy.

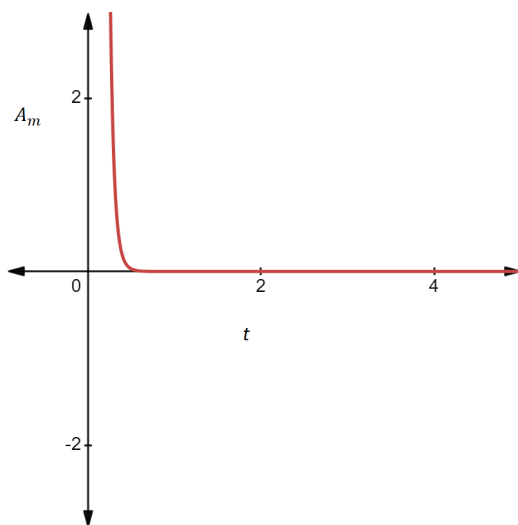


Figure 3. Plotting the anisotropic parameter vs cosmic time (t) for $n = 1.1$ and $k = 1$

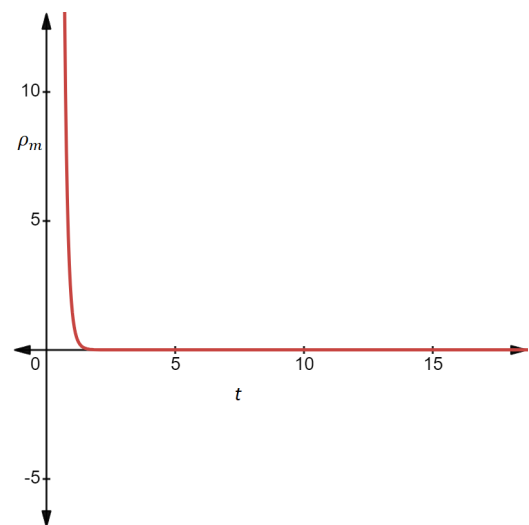


Figure 4. Plotting the matter energy density vs cosmic time (t) for $c_1 = 100$, $n = 1.1$ and $k = 1$

Using equation (34), from equations (12) and (3), we obtain

$$\rho_m = c_1 t^{-\frac{3k}{n}} e^{-\frac{3t}{n}} \quad (40)$$

where c_1 is the integration constant.
And

$$\rho_{BHDE} = 3 \left(\alpha \left(\frac{k+t}{nt} \right)^2 + \beta \left(\frac{-k}{nt^2} \right)^{\frac{2-\Delta}{2}} \right) \quad (41)$$

We can see that both the energy densities are decreasing functions of cosmic time t . The evolution of the matter energy density (ρ_m) is shown in Figure 4, showing that it is large in the early stages of the universe and tends to zero in the later stages. For $\Delta = 0$, the BHDE density provided by equation (41) behaves like the standard HDE. A different cosmic scenario will arise from the deviation of BHDE's behavior from the standard one, contingent on the Δ parameter. Plotting

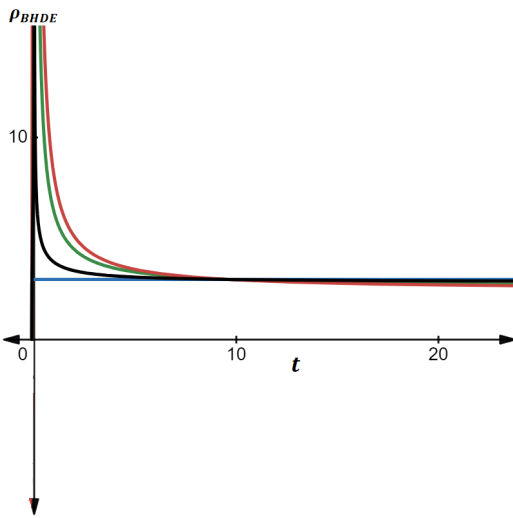


Figure 5. Plotting the Barrow HDE density vs cosmic time (t) for $\alpha = 1, \beta = 0.7$ with $\Delta = 0$ (Red solid line), $\Delta = 0.5$ (Green solid line), $\Delta = 1.5$ (Black solid line) and $\Delta = 2$ (Blue solid line)

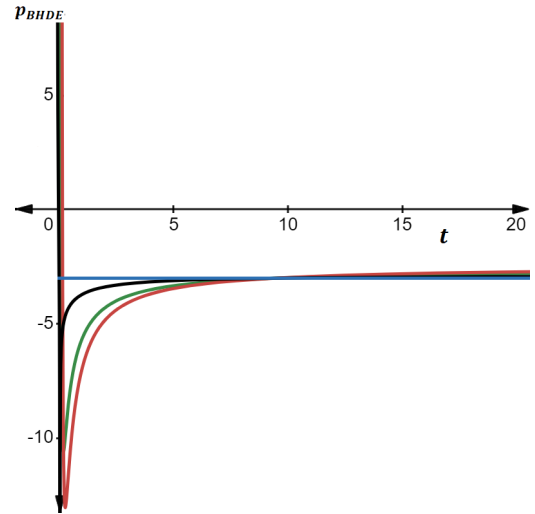


Figure 6. Plotting the Barrow HDE pressure p_{BHDE} vs cosmic time (t) for $\alpha = 1, \beta = 0.7$ with $\Delta = 0$ (Red solid line), $\Delta = 0.5$ (Green solid line), $\Delta = 1.5$ (Black solid line) and $\Delta = 2$ (Blue solid line)

BHDE against cosmic time t for various values of Δ allows us to comprehend its evolution. Figure 5 illustrates that the BHDE density decreases as cosmic time t increases for values of $\Delta = 0, 0.5$ and 1.5 , and eventually tends to a constant value. The BHDE density, on the other hand, remains constant throughout the evolution of the universe for $\Delta = 2$. In this case, the model is referred to as the Λ CDM model, and the BHDE acts like a cosmological constant. Volume of the universe is increasing, according to the physical consequences of the decline in energy densities.

We obtain pressure p_{BHDE} of the Barrow HDE as follows by using equations (34) and (41) in equation (13) as

$$p_{BHDE} = - \left[\alpha \left(\frac{k+t}{nt} \right)^2 + \beta \left(\frac{-k}{nt^2} \right) \right]^{\frac{-\Delta}{2}} \left[\frac{(2-\Delta)nt}{k+n} \left(-\alpha k \left(\frac{n+k}{n^2 t^3} \right) + \frac{\beta k}{nt^3} \right) + 3 \left(\alpha \left(\frac{k+t}{nt} \right)^2 + \beta \left(\frac{-k}{nt^2} \right) \right) \right] \quad (42)$$

Equation (42) gives the Barrow holographic dark energy pressure (p_{BHDE}) with respect to cosmic time t , which is shown in Figure 6. For $\Delta = 0, 0.5$ and 1.5 , the pressure p_{BHDE} is extremely negative at the beginning and rises gradually as cosmic time t increases until it reaches a certain constant value. However for $\Delta = 2$, the pressure is constantly negative in the entire evolution of the universe. This indicates that the universe is undergoing accelerated expansion for all the values of Δ , as the pressure remains negative throughout the evolution.

Equation of state parameter (EoS parameter) ω_{BHDE} of Barrow HDE is determined as follows by using equations (41) and (42).

$$\omega_{BHDE} = \frac{p_{BHDE}}{\rho_{BHDE}} = -1 + \frac{(\Delta - 2) \frac{k}{nt^2} \left(\frac{\beta}{t} - \alpha \left(\frac{k+t}{nt} \right) \right)}{\left(\frac{k+t}{nt} \right) \left[\alpha \left(\frac{k+t}{nt} \right)^2 - \frac{\beta k}{nt^2} \right]} \quad (43)$$

According to equation (43), when $\Delta < 2$, the EoS parameter ω_{BHDE} in our model is a strictly decreasing function of cosmic time t . For various values of Δ , Figure 7 shows how the EoS parameter ω_{BHDE} varies with cosmic time t . The graph shows that, after a specific point in time throughout its evolution, initially the EoS parameter ω_{BHDE} in our model varies in the quintessence region $\left(-1 < \omega_{BHDE} < -\frac{1}{3} \right)$ for $\Delta = 0, 0.5$, and 1.5 and after 5 billion years (approx), the EoS parameter ω_{BHDE} eventually approaches the Λ CDM ($\omega_{BHDE} = -1$) model as it converges to -1 at late times. With $\Delta = 2$, the evolution of the EoS parameter ω_{BHDE} never changes and always has a value of -1 . The Barrow holographic dark energy behaves like the cosmological constant Λ , as was previously mentioned. After taking into account every scenario in our model, we can say that the expansion rate will accelerate more with large values of cosmic time t .

The total energy density is obtained from equations (34), (40) and (41) as

$$\Omega = \frac{\rho_m}{3H^2} + \frac{\rho_{BHDE}}{3H^2} = \Omega_m + \Omega_{BHDE}$$

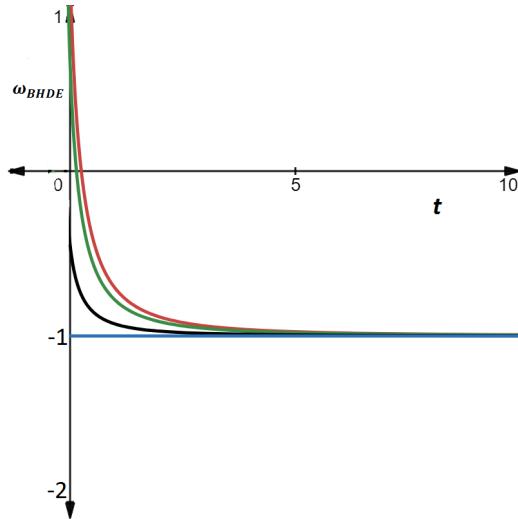


Figure 7. Plotting the equation of state parameter (EoS parameter) ω_{BHDE} vs cosmic time (t) for $\alpha = 1, \beta = 0.7$ with $\Delta = 0$ (Red solid line), $\Delta = 0.5$ (Green solid line), $\Delta = 1.5$ (Black solid line) and $\Delta = 2$ (Blue solid line)

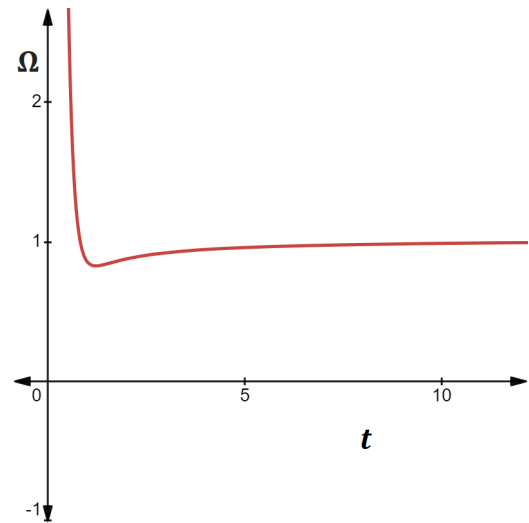


Figure 8. Plotting the total energy density parameter (Ω) vs cosmic time (t) for $\alpha = 1, \beta = 0.7, c_1 = 100$ with $\Delta = 0.5$

$$= \frac{c_1 t^{-\frac{3k}{n}} e^{-\frac{3t}{n}}}{3 \left(\frac{k+t}{nt}\right)^2} + \frac{\left(\alpha \left(\frac{k+t}{nt}\right)^2 + \beta \left(\frac{-k}{nt^2}\right)\right)^{\frac{2-\Delta}{2}}}{\left(\frac{k+t}{nt}\right)^2} \quad (44)$$

The total energy density Ω varies throughout cosmic time t as seen in the graph shown in Figure 8. The parameters denoting the total energy density, $\Omega > 1$, $\Omega = 1$, and $\Omega < 1$, respectively, correspond to the open, flat, and closed universe. The overall density parameter Ω decreases with time, as the figure shows. The universe eventually becomes flat at later times, as indicated by the total density parameter Ω eventually approaching 1.

4.1. Jerk parameter (j)

The universe's acceleration, or how quickly the rate of expansion is changing throughout cosmic time t , is measured by the cosmic jerk parameter, j . It is a dimensionless quantity that gives crucial information on the universe's expansion and is defined as the third derivative of the scale factor a with respect to cosmic time t . The universe transitions from an era of decelerated expansion to one of accelerated expansion, when the jerk parameter, j , is positive. The jerk parameter j for the widely used Λ CDM model has a value of one.

The jerk parameter j is defined mathematically as

$$j = \frac{1}{aH^3} \frac{d^3 a}{dt^3} \quad (45)$$

We derive the jerk parameter j for our model as

$$j = \frac{\left(\frac{1}{n}\right)^3 + \frac{3k}{n^3} + \frac{3k}{n^2} \left(\frac{k}{n} - 1\right) + \frac{k}{n} \left\{ \left(\frac{k}{n}\right)^2 - 3\left(\frac{k}{n}\right) + 2 \right\}}{\left(\frac{t+k}{nt}\right)^3} \quad (46)$$

Figure 9 displays the graph of the jerk parameter j . It is clear from the figure that the jerk parameter j stays positive during the universe's evolution, indicating a growing rate of expansion. Furthermore, figure 9 shows that the jerk parameter j converges to 1 at late times, suggesting that the model mimics the behavior of the Λ CDM model.

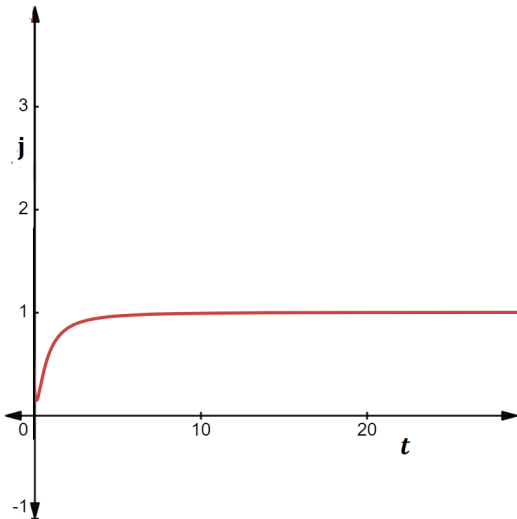


Figure 9. Plotting the jerk parameter vs cosmic time (t) for $n = 1.1$ and $k = 1$

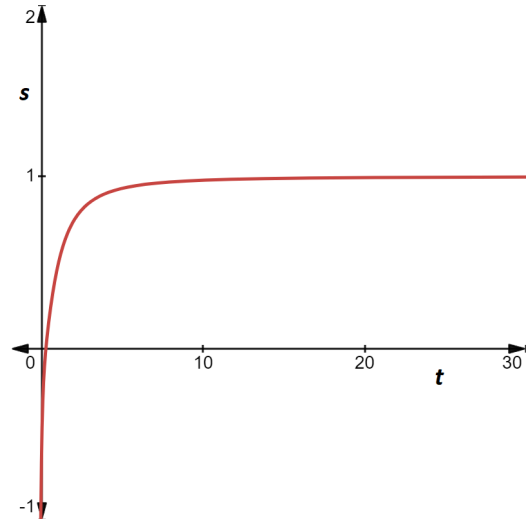


Figure 10. Plotting the snap parameter vs cosmic time (t) for $n = 1.1$ and $k = 1$

4.2. Snap parameter(s):

The fourth order derivative of the scale factor a with respect to cosmic time t is known as the snap parameter (s), a dimensionless quantity. It aids in understanding the dynamics of the universe by describing the pace at which the acceleration of the universe's expansion is changing. Mathematically, the snap parameter (s) is defined as

$$s = \frac{1}{aH^4} \frac{d^4 a}{dt^4} \tag{47}$$

The snap parameter (s) for our model is found as

$$s = \frac{\left(\frac{1}{n}\right)^4 + \frac{4k}{n^4} + \frac{6k}{n^3} \left(\frac{k}{n} - 1\right) + \frac{4k}{n^2} \left(\left(\frac{k}{n}\right)^2 - 3\left(\frac{k}{n}\right) + 2\right) + \frac{\left(\frac{k}{n}\right)^4 - 6\left(\frac{k}{n}\right)^3 + 11\left(\frac{k}{n}\right)^2 - 6\left(\frac{k}{n}\right)}{t^4}}{\left(\frac{k+t}{nt}\right)^4} \tag{48}$$

The variation of the snap parameter s with respect to cosmic time t is shown in Figure 10. The increasing behavior is displayed by the snap parameter (s). It is negative when $t \rightarrow 0$ and increases with cosmic time t . Eventually, the snap parameter s converges to 1 at late times. This indicates an accelerated expansion phase of the universe.

4.3. Lerk parameter(l):

Another dimensionless quantity is the lerk parameter l , which is the fifth order derivative of the scale factor a with respect to cosmic time t .

The lerk parameter l is described mathematically as

$$l = \frac{1}{aH^5} \frac{d^5 a}{dt^5} \tag{49}$$

We derive the lerk parameter l for our model as

$$l = \frac{\left(\frac{1}{n}\right)^5 + \frac{5k}{n^5} + \frac{10k}{n^4} \left(\frac{k}{n} - 1\right) + \frac{10\left(\frac{k}{n^3}\right) \left(\left(\frac{k}{n}\right)^2 - 3\left(\frac{k}{n}\right) + 2\right) + 5\left(\frac{k}{n^2}\right) \left(\left(\frac{k}{n}\right)^3 - 6\left(\frac{k}{n}\right)^2 + 11\left(\frac{k}{n}\right) - 6\right) + \frac{\left(\frac{k}{n}\right)^5 - 10\left(\frac{k}{n}\right)^4 + 35\left(\frac{k}{n}\right)^3 - 50\left(\frac{k}{n}\right)^2 + 24\left(\frac{k}{n}\right)}{t^5}}{\left(\frac{t+k}{nt}\right)^5} \tag{50}$$

The variation of the lerk parameter l with respect to cosmic time t is shown in Figure 11. The figure illustrates that the lerk parameter, l , is high at $t \rightarrow 0$ and decreases progressively as cosmic time t , increases. At late times, it converges to 1.

4.4. Energy conditions:

In the context of general relativity, energy conditions are a collection of theoretical inequalities which operate as linear combinations of energy density and pressure that describe the behavior of energy and matter in a given spacetime. These conditions are derived from the Einstein field equations of general relativity and play a crucial role in understanding the properties and evolution of the universe. They often place constraints on the possible forms of energy and matter that can exist in the universe. There are several types of energy conditions, each with its own implications for the nature of matter and energy in the universe. The null energy condition (NEC), the weak energy condition (WEC), the strong energy condition (SEC), and the dominant energy condition (DEC) are the linear energy conditions among them.

The four energy conditions are as follows:

$$\text{Null energy condition(NEC)} \Leftrightarrow (\rho + p) \geq 0 \quad (51)$$

$$\text{Weak energy condition(WEC)} \Leftrightarrow (\rho \geq 0) \text{ and } (\rho + p \geq 0) \quad (52)$$

$$\text{Strong energy condition(SEC)} \Leftrightarrow (\rho + 3p \geq 0) \text{ and } (\rho + p \geq 0) \quad (53)$$

$$\text{Dominant energy condition(DEC)} \Leftrightarrow (\rho \geq 0) \text{ and } (\rho \pm p \geq 0) \quad (54)$$

For our model,

$$\rho = \rho_m + \rho_{BHDE} \quad \text{and} \quad p = p_{BHDE}$$

consequently,

$$\rho + p = c_1 t^{\frac{-3k}{n}} e^{\frac{-3t}{n}} - \left(\alpha \left(\frac{k+t}{nt} \right)^2 + \beta \left(\frac{-k}{nt^2} \right) \right)^{-\frac{\Delta}{2}} \cdot \left[\frac{(2-\Delta)nt}{k+n} \left\{ -\alpha k \left(\frac{n+k}{n^2 t^3} \right) + \frac{\beta k}{nt^3} \right\} \right] \quad (55)$$

$$\rho - p = c_1 t^{\frac{-3k}{n}} e^{\frac{-3t}{n}} + \left(\alpha \left(\frac{k+t}{nt} \right)^2 + \beta \left(\frac{-k}{nt^2} \right) \right)^{-\frac{\Delta}{2}} \cdot \left[\frac{(2-\Delta)nt}{k+n} \left\{ -\alpha k \left(\frac{n+k}{n^2 t^3} \right) + \frac{\beta k}{nt^3} \right\} + 6 \left\{ \alpha \left(\frac{k+t}{nt} \right)^2 - \frac{\beta k}{nt^2} \right\} \right] \quad (56)$$

$$\rho + 3p = c_1 t^{\frac{-3k}{n}} e^{\frac{-3t}{n}} - 3 \left(\alpha \left(\frac{k+t}{nt} \right)^2 + \beta \left(\frac{-k}{nt^2} \right) \right)^{-\frac{\Delta}{2}} \cdot \left[\frac{(2-\Delta)nt}{k+n} \left\{ -\alpha k \left(\frac{n+k}{n^2 t^3} \right) + \frac{\beta k}{nt^3} \right\} + 2 \left\{ \alpha \left(\frac{k+t}{nt} \right)^2 - \frac{\beta k}{nt^2} \right\} \right] \quad (57)$$

However, the SEC is known to be violated in an accelerated expansion phase of the universe. Figure 12 shows a plot of the energy conditions, which indicates that in our model, initially, the NEC, WEC, SEC and DEC are all satisfied, but at late times, the SEC gets violated. The violation of the SEC results in the acceleration of the universe.

4.5. Coincidence parameter (\bar{r}):

The coincidence parameter, symbolized by \bar{r} , is a measure representing the ratio between two energy densities within the universe, namely $\bar{r} = \frac{\rho_{BHDE}}{\rho_m}$. According to current data, the coincidence parameter's value must either stay constant or vary very slowly as the universe expands. However, the simplest and most widely acknowledged dark energy model, the Λ CDM model, doesn't align with these observations. Numerous different models are therefore taken into consideration to get over this problem of coincidence.

The coincidence parameter (\bar{r}) for our model can be found as

$$\bar{r} = \frac{3 \left(\alpha \left(\frac{k+t}{nt} \right)^2 + \beta \left(\frac{-k}{nt^2} \right) \right)^{\frac{2-\Delta}{2}}}{c_1 t^{\frac{-3k}{n}} e^{\frac{-3t}{n}}} \quad (58)$$

The graph in Figure 13 illustrates the change in the coincidence parameter \bar{r} over cosmic time t . It's evident that \bar{r} increases rapidly in later stages, indicating that our model doesn't resolve the coincidence problem. As we've assumed no interaction between BHDE and dark matter, exploring an interacting model could be insightful. Therefore, a specific form

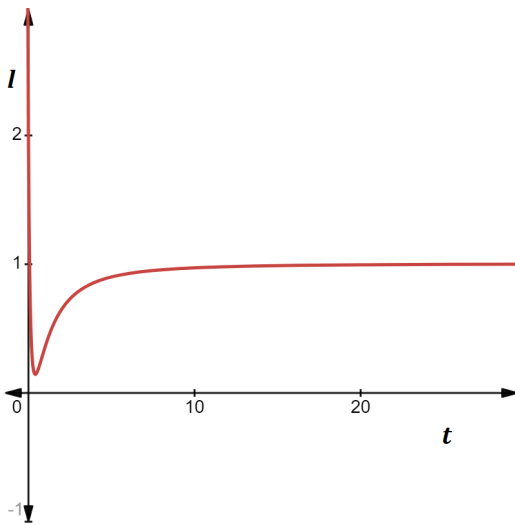


Figure 11. Plotting the lerk parameter vs cosmic time (t) for $n = 1.1$ and $k = 1$

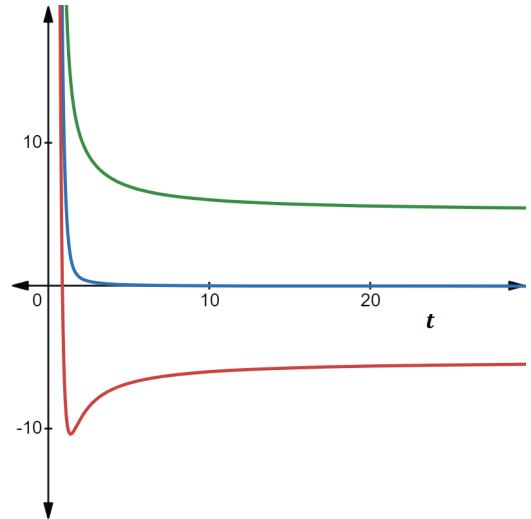


Figure 12. Plotting the energy conditions vs cosmic time (t) for $n = 1.1, k = 1, c_1 = 100, \Delta = 0.5, \alpha = 1, \beta = 0.7, \rho + p$ (blue line), $\rho - p$ (green line), $\rho + 3p$ (red line)

of interaction between Barrow holographic dark energy and dark matter might keep their density ratios relatively constant over the course of the universe’s evolution.

5. STATEFINDER DIAGNOSTIC

In order to differentiate between different dark energy-related cosmological scenarios, a precise and robust method for evaluating DE models is important. In order to do this, Sahni *et al.* [32] proposed the Statefinder diagnostic, that uses the parameter pair $\{r, s\}$. Different dark energy models, including the cosmological constant, quintessence, Chaplygin gas, braneworld models, and models with interacting dark energy, can be effectively distinguished by the pair. The construction of the dimensionless Statefinder diagnostic involves taking into account the universe’s scale factor a and its higher order derivative just with regard to cosmic time t . The parameter r represents the hierarchy of geometrical cosmological parameters, succeeding the Hubble parameter H and the deceleration parameter q . The parameter s , on the other hand, is independent of the density associated to dark energy as it is obtained as a linear combination of q and r . The definition of the Statefinder diagnostic pair $\{r, s\}$ is

$$r = \frac{1}{aH^3} \frac{d^3 a}{dt^3} \quad \text{and} \quad s = \frac{r - 1}{3(q - \frac{1}{2})}, \quad \text{where} \quad q \neq \frac{1}{2} \tag{59}$$

In case of our model, r and s are found to be as

$$r = \frac{\left(\frac{1}{n}\right)^3 + \frac{3k}{n^3} + \frac{3k}{n^2} \frac{(k-1)}{t^2} + \frac{k}{n} \left\{ \left(\frac{k}{n}\right)^2 - 3\left(\frac{k}{n}\right) + 2 \right\}}{\left(\frac{t+k}{nt}\right)^3} \tag{60}$$

$$s = \frac{-6\left(\frac{k}{n^2}\right)t - 6\left(\frac{k}{n}\right)^2 + 4\left(\frac{k}{n}\right)}{3\left(\frac{1}{n}\right)(t+k) \left\{ 2\left(\frac{k}{n}\right) - 3\left(\frac{1}{n}t + \frac{k}{n}\right)^2 \right\}} \tag{61}$$

For these cosmological parameters, the $r - s$ plane is $(1, 0)$ for Λ CDM and $(1, 1)$ for standard CDM(SCDM). While the trajectories for Chaplygin gas are located in the range $(r > 1, s < 0)$, the quintessential dark energy epochs are represented by the region $(r < 1, s > 0)$. The Statefinder diagnostic pair in our model is dependent on the cosmic time t , as shown by equations (60) and (61). The diagnostic pair results in $r = 1$ and $s = 0$ as t approaches infinity. Additionally, figure 14 verifies that later stages of our model coincide with the Λ CDM model.

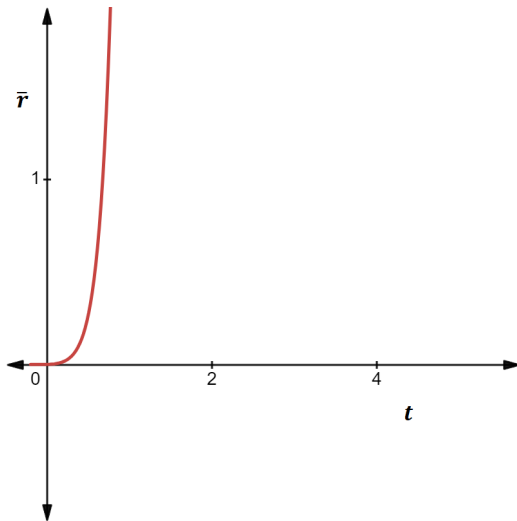


Figure 13. Plotting the coincidence parameter vs cosmic time (t) for $n = 1.1, k = 1, c_1 = 100, \Delta = 0.5, \alpha = 1, \beta = 0.7$

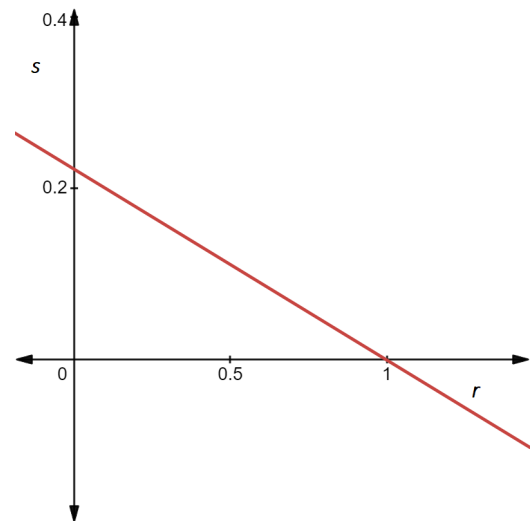


Figure 14. Plotting the statefinder parameters s vs r (t) for $n = 1.1$ and $k = 1$

6. CORRESPONDENCE BETWEEN THE BARROW HOLOGRAPHIC DARK ENERGY MODEL AND QUINTESSENCE SCALAR FIELD MODEL

To establish correspondence between holographic dark energy with quintessence dark energy models, we compare their equations of state and dark energy densities. For the universe to undergo accelerated expansion, the equation of state parameter for quintessence must be less than $-\frac{1}{3}$.

The energy density and pressure for the quintessence scalar field model are defined by:

$$\rho_\phi = \frac{\dot{\phi}^2}{2} + V(\phi) \quad (62)$$

$$p_\phi = \frac{\dot{\phi}^2}{2} - V(\phi) \quad (63)$$

where ϕ represents the quintessence scalar field and $V(\phi)$ denotes the potential of the scalar field ϕ . The equation of state parameter for the scalar field is expressed as

$$\omega_\phi = \frac{p_\phi}{\rho_\phi} = \frac{\dot{\phi}^2 - 2V(\phi)}{\dot{\phi}^2 + 2V(\phi)} \quad (64)$$

Equations (62) and (63) provide

$$\dot{\phi}^2 = \rho_\phi + p_\phi \quad (65)$$

$$V(\phi) = \frac{\rho_\phi - p_\phi}{2} \quad (66)$$

By using equations (43) and (64), we obtain

$$-1 + \frac{(\Delta - 2) \frac{k}{nt^2} \left(\frac{\beta}{t} - \alpha \left(\frac{k+t}{nt} \right) \right)}{\left(\frac{k+t}{nt} \right) \left[\alpha \left(\frac{k+t}{nt} \right)^2 - \frac{\beta k}{nt^2} \right]} = \frac{\dot{\phi}^2 - 2V(\phi)}{\dot{\phi}^2 + 2V(\phi)} \quad (67)$$

By equating ρ_ϕ with ρ_{BHDE} and p_ϕ with p_{BHDE} , we can compute the kinetic energy $\dot{\phi}^2$ and the scalar potential $V(\phi)$ as

$$\dot{\phi}^2 = - \left[\alpha \left(\frac{k+t}{nt} \right)^2 + \beta \left(\frac{-k}{nt^2} \right) \right]^{\frac{-\Delta}{2}} \left[\frac{(2-\Delta)}{k+n} \left(-\alpha k \left(\frac{n+k}{nt^2} \right) + \frac{\beta k}{t^2} \right) \right] \quad (68)$$

$$V(\phi) = 3 \left[\alpha \left(\frac{k+t}{nt} \right)^2 + \beta \left(\frac{-k}{nt^2} \right) \right]^{\frac{2-\Delta}{2}} + \frac{1}{2} \left[\alpha \left(\frac{k+t}{nt} \right)^2 + \beta \left(\frac{-k}{nt^2} \right) \right]^{\frac{-\Delta}{2}} \left[\frac{(2-\Delta)}{k+n} \left(-\alpha k \left(\frac{n+k}{nt^2} \right) + \frac{\beta k}{t^2} \right) \right] \quad (69)$$

Thus, we have determined the potential $V(\phi)$ and the scalar field ϕ for the quintessence scalar field model corresponding to the BHDE model. The kinetic energy $\dot{\phi}^2$ is shown in Figure 15, illustrating that it decreases over cosmic time t and eventually diminishes at late times. Figure 16 depicts the scalar field potential $V(\phi)$ for the quintessence model, indicating that $V(\phi)$ also decreases over cosmic time t and tends to a constant value at late times. This type of potential and kinetic energy can lead to the accelerated expansion of the universe.

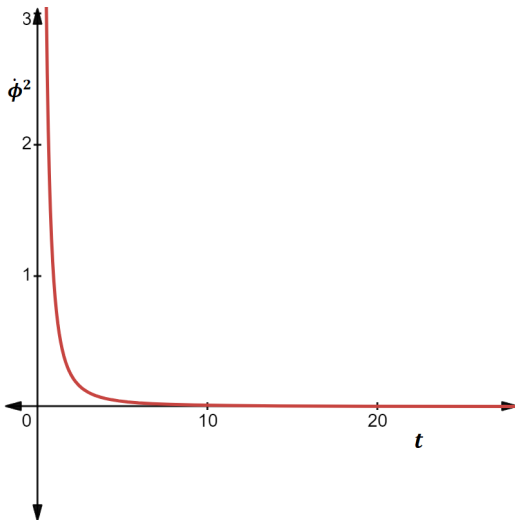


Figure 15. Plotting the kinetic energy $\dot{\phi}^2$ vs (t) for $n = 1.1, k = 1, \Delta = 0.5, \alpha = 1$ and $\beta = 0.7$

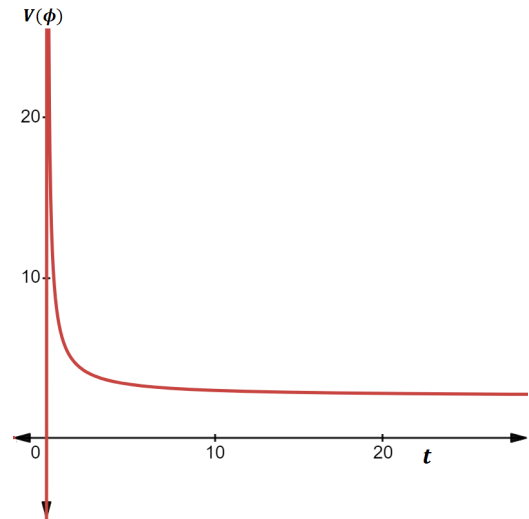


Figure 16. Plotting the potential energy $V(\phi)$ vs (t) for $n = 1.1, k = 1, \Delta = 0.5, \alpha = 1$ and $\beta = 0.7$

7. CONCLUSION

In this study, we consider Barrow holographic dark energy with Granda - Oliverso length scale as the infrared cutoff to construct a spatially homogeneous and anisotropic Bianchi type-V universe within the framework of General Relativity. The universe is assumed to be filled with a mixture of cold dark matter and the Barrow holographic dark energy which does not interact with the cold dark matter. Exact solution of the Einstein field equations are obtained by imposing the condition that the average scale factor a obeys a hybrid expansion law. We then investigate the physical and kinematic characteristics of the model by analyzing its parameters of cosmological importance and find that:

- At time $t \rightarrow 0$, the volume V of the universe is zero, indicating that the universe starts from a point of zero volume and expands throughout its evolution. This suggests that the universe began with a Big Bang singularity.
- The universe transitions from an early deceleration phase to a recent acceleration phase, as illustrated in Figure 2, and this aligns well with recent observations.
- The Hubble parameter H , the expansion scalar θ , and the shear scalar σ each diverges at $t \rightarrow 0$, and then all decrease with increasing cosmic time t but remains positive.
- The anisotropic parameter A_m approaches zero for sufficiently large time. Thus, the present model becomes isotropic at late times.
- The matter energy density ρ_m and the Barrow holographic dark energy density ρ_{BHDE} both decrease as cosmic time t increases. This decrease in energy densities over time results in the expansion of the universe.
- In later epochs, the pressure of Barrow holographic dark energy p_{BHDE} becomes negative, indicating the universe's accelerated expansion.
- In the beginning, the equation of state parameter ω_{BHDE} for Barrow holographic dark energy experiences variation within the quintessence region, gradually approaching the Λ CDM model as time progresses.

- The total energy density parameter Ω tends to 1 as $t \rightarrow \infty$. This implies that the universe is approaching towards a flat universe in its later stage.
- The Null energy condition, Weak energy condition, and Dominant energy condition are all satisfied, but in the later stages, the Strong energy condition is violated, indicating the universe's accelerated expansion.
- The cosmic jerk parameter (j), snap parameter (s), and lerk parameter (l) all approach the value 1 as time progresses. This convergence, particularly of j , indicates that our model aligns with the Λ CDM model at late time.
- Throughout the evolution of the universe, the coincidence parameter, \bar{r} varies. In our model, the coincidence problem remains unresolved.
- The Statefinder parameters intersect at the point (1, 0), signifying alignment with the Λ CDM model.
- The correlation between the Barrow holographic dark energy model and the quintessence scalar field model explains the accelerated expansion phase of the universe.

ORCID

 **Chandra Rekha Mahanta**, <https://orcid.org/0000-0002-8019-8824>;  **Rajashree Mahanta**, <https://orcid.org/0009-0009-2656-115X>;  **Joy Prakash Medhi**, <https://orcid.org/0009-0004-5275-5330>

REFERENCES

- [1] A.G. Riess, *et al.*, "Observational evidence from supernovae for an accelerating universe and a cosmological constant," *The Astronomical Journal*, **116**, 1009-1038 (1998). <https://doi.org/10.1086/300499>
- [2] S. Perlmutter, *et al.*, "Measurements of Ω and Λ from 42 high-redshift supernovae," *The Astrophysical Journal*, **517**, 565-586 (1999). <https://doi.org/10.1086/307221>
- [3] D.N. Spergel, *et al.*, "First-year Wilkinson Microwave Anisotropy Probe (WMAP) observations: Determination of cosmological parameters," *Astrophys. J. Suppl. Ser.* **148**, 175-194 (2003). <https://doi.org/10.1086/377226>
- [4] D.N. Spergel, *et al.*, "Three-Year Wilkinson Microwave Anisotropy Probe (WMAP) Observations: Implications for Cosmology," *Astrophys. J. Suppl. Ser.* **170**, 377 (2007). <https://doi.org/10.1086/513700>
- [5] E. Komatsu, *et al.*, "Five-Year Wilkinson Microwave Anisotropy Probe observation: cosmological interpretation," *Astrophys. J. Suppl. Ser.* **180**, 330 (2009). <https://doi.org/10.1088/0067-0049/180/2/330>
- [6] M. Tegmark, *et al.*, "Cosmological parameters from SDSS and WMAP," *Phys. Rev. D*, **69**, 103501 (2004). <https://doi.org/10.1103/PhysRevD.69.103501>
- [7] U. Seljak, *et al.*, "Cosmological parameter analysis including SDSS Ly α forest and galaxy bias: constraints on the primordial spectrum of fluctuations, neutrino mass, and dark energy," *Phys. Rev. D*, **71**, 103515 (2005). <https://doi.org/10.1103/PhysRevD.71.103515>
- [8] M. Tegmark, *et al.*, "Cosmological constraints from the SDSS luminous red galaxies," *Phys. Rev. D*, **74**, 123507 (2006). <https://doi.org/10.1103/PhysRevD.74.123507>
- [9] D.J. Eisenstein, *et al.*, "Detection of the Baryon Acoustic Peak in the Large-Scale correlation function of SDSS luminous red galaxies," *The Astronomical Journal*, **633**, 560-574 (2005). <https://doi.org/10.1086/466512>
- [10] P.J.E Peebles and Bharat Ratra, "The cosmological constant and dark energy," *Rev. Mod. Phys.* **75**, 559 (2003). <https://doi.org/10.1103/RevModPhys.75.559>
- [11] Planck Collaboration, "Planck 2018 results VI. Cosmological parameters," *A&A*, **641**, A6 (2020). <https://doi.org/10.1051/0004-6361/201833910>
- [12] Edmund J. Copeland, "Dynamics of Dark Energy," *AIP Conf. Proc.* **957**, 21-29 (2007). <https://doi.org/10.1063/1.2823765>
- [13] G.'t Hooft, "Dimensional reduction in quantum gravity," *arXiv.gr-qc/9310026* (2009). <https://doi.org/10.48550/arXiv.gr-qc/9310026>
- [14] A.G. Cohen, D.B. Kaplan, and A.E. Nelson, "Effective Field Theory, Black Holes, and the Cosmological Constant," *Phys. Rev. Lett.* **82**, 4971-4974 (1999). <https://doi.org/10.1103/PhysRevLett.82.4971>
- [15] P. Hořava, and D. Minic, "Probable Values of the Cosmological Constant in a Holographic Theory," *Phys. Rev. Lett.* **85**, 1610-1613 (2000). <https://doi.org/10.1103/PhysRevLett.85.1610>
- [16] S.D.H. Hsu, "Entropy bounds and dark energy," *Phys. Lett. B*, **594**, 13 (2004). <https://doi.org/10.1016/j.physletb.2004.05.020>
- [17] M. Li, "A model of holographic dark energy," *Phys. Lett. B*, **603**, 1-5 (2004). <https://doi.org/10.1016/j.physletb.2004.10.014>
- [18] L.N. Granda, and A. Oliveros, "Infrared cut-off proposal for the holographic density," *Phys. Lett. B*, **669**(5), 275-277 (2008). <https://doi.org/10.1016/j.physletb.2008.10.017>
- [19] M. Tavayef, A. Sheykhi, K. Bamba, and H. Moradpour, "Tsallis holographic dark energy," *Phys. Lett. B*, **781**, 195-200 (2018). <https://doi.org/10.1016/j.physletb.2018.04.001>

- [20] C. Tsallis, and L.J.L. Cirto, "Black hole thermodynamical entropy," *Eur. Phys. J. C*, **73**, 2487 (2013). <https://doi.org/10.1140/epjcs10052-013-2487-6>
- [21] H. Moradpour, *et al.*: "Thermodynamic approach to holographic dark energy and the Rényi entropy," *Eur. Phys. J. C*, **78**, 829 (2018). <https://doi.org/10.1140/epjcs10052-018-6309-8>
- [22] J.D. Barrow, "The area of a rough black hole," *Phys. Lett. B*, **808**, 135643 (2020). <https://doi.org/10.1016/j.physletb.2020.135643>
- [23] S. Wang, Y. Wang, and M. Li, "Holographic dark energy," *Phys. Rep.* **696**, 1–57 (2017). <https://doi.org/10.1016/j.physrep.2017.06.003>
- [24] E.N. Saridakis, "Barrow holographic dark energy," *Phys. Rev. D*, **102**, 123525 (2020). <https://doi.org/10.1103/PhysRevD.102.123525>
- [25] S. Srivastava, and U.K. Sharma, "Barrow holographic dark energy with Hubble horizon as IR cutoff," *Int. J. Geo. Methods in Mod. Phys.* **18**, 2150014 (2021). <https://doi.org/10.1142/S0219887821500146>
- [26] N. K. P and T. K. Mathew, "Barrow Holographic Dark Energy Model with GO Cut-off – An Alternative Perspective," <https://doi.org/10.48550/arXiv.2112.07310>
- [27] A. Oliverosa, M.A. Sabogal, M.A. Acero, "Barrow holographic dark energy with Granda–Oliveros cutoff," *Eur. Phys. J. Plus*, **137**, 783 (2022). <https://doi.org/10.1140/epjp/s13360-022-02994-z>
- [28] B.C. Paul, *et al.*, "Bianchi-I anisotropic universe with Barrow holographic dark energy," *Eur. Phys. J. C*, **82**, 76 (2022). <https://doi.org/10.1140/epjcs10052-022-10041-5>
- [29] C.L. Bennett *et al.*, "The Microwave Anisotropy Probe* Mission," *The Astrophysical Journal*, **583**, 1-23 (2003). <https://doi.org/10.1086/345346>
- [30] Bernardis, *et al.*, "MAXIMA-1: A Measurement of the Cosmic Microwave Background Anisotropy on Angular Scales of 10'–5°," *The Astrophysical Journal*, **545**, (2000). <https://doi.org/10.1086/317322>
- [31] G. Hinshaw *et al.*, "Five-Year Wilkinson Microwave Anisotropy Probe* Observations: Data Processing, Sky Maps, and Basic Results," *The Astrophysical Journal Supplement Series*, **180**, 225–245 (2009). <https://doi.org/10.1088/0067-0049/180/2/225>
- [32] V. Sahni, T.D. Saini, A.A. Starobinsky, and U. Alam, "Statefinder—a new geometrical diagnostic of dark energy," *JETP Lett.* **77**, 201-206 (2003). <https://doi.org/10.1134/1.1574831>

КОСМІЧНА ЕВОЛЮЦІЯ У ВСЕСВІТІ БІАНКІ ТИПУ V З ГОЛОГРАФІЧНОЮ ТЕМНОЮ ЕНЕРГІЄЮ БАРРОУ ЗІ ШКАЛОЮ ДОВЖИНИ ГРАНДА-ОЛІВЕРОСА ЯК ІЧ ВІДСІЧЕННЯ

Чандра Рекха Маханга, Раджашрі Маханга, Джой Пракаш Медхі

Факультет математики, Університет Гаухаті, Гувахаті - 781014, Індія

У цій роботі ми будемо просторово однорідну та анізотропну космологічну модель типу Б'янки V із гібридним законом розширення, розглядаючи Всесвіт як заповнений холодною темною матерією та незв'язаною голографічною темною енергією Барроу зі шкалою довжини Гранда-Олівероса як ІЧ-відсічення. Фізичні та кінематичні характеристики отриманої моделі обговорюються шляхом вивчення еволюції різних параметрів космологічного значення, таких як параметр Хаббла, параметр уповільнення, анізотропний параметр, параметр рівняння стану, параметр ривка тощо. Ми також досліджуємо, чи енергетичні умови виконуються або порушуються. Наш аналіз показує, що умови нульової, слабкої та домінуючої енергії виконуються, тоді як умова сильної енергії порушена, що підтримує прискорене розширення Всесвіту. Діагностика вимірювача стану також була виконана на основі останніх космологічних спостережень, щоб порівняти нашу модель з різними космологічними сценаріями темної енергії. Крім того, ми встановлюємо відповідність між квінтесенційним скалярним полем і голографічною моделлю темної енергії Барроу, що підтверджує наш опис прискореного розширення Всесвіту.

Ключові слова: космічне прискорення; голографічна темна енергія Барроу; Біанкі тип-V; холодна темна матерія; параметр уповільнення; рівняння параметра стану